NASA/TM—2002-211104

Ultrasonic Resonance Spectroscopy of Composite Rims for Flywheel Rotors

Laura M. Harmon
Cleveland State University, Cleveland, Ohio

George Y. Baaklini
Glenn Research Center, Cleveland, Ohio

September 2002

The NASA STI Program Office . . . in Profile

Since its founding, NASA has been dedicated to the advancement of aeronautics and space science. The NASA Scientific and Technical Information (STI) Program Office plays a key part in helping NASA maintain this important role.

The NASA STI Program Office is operated by Langley Research Center, the Lead Center for NASA's scientific and technical information. The NASA STI Program Office provides access to the NASA STI Database, the largest collection of aeronautical and space science STI in the world. The Program Office is also NASA's institutional mechanism for disseminating the results of its research and development activities. These results are published by NASA in the NASA STI Report Series, which includes the following report types:

- TECHNICAL PUBLICATION. Reports of completed research or a major significant phase of research that present the results of NASA programs and include extensive data or theoretical analysis. Includes compilations of significant scientific and technical data and information deemed to be of continuing reference value. NASA's counterpart of peer-reviewed formal professional papers but has less stringent limitations on manuscript length and extent of graphic presentations.

- TECHNICAL MEMORANDUM. Scientific and technical findings that are preliminary or of specialized interest, e.g., quick release reports, working papers, and bibliographies that contain minimal annotation. Does not contain extensive analysis.

- CONTRACTOR REPORT. Scientific and technical findings by NASA-sponsored contractors and grantees.

- CONFERENCE PUBLICATION. Collected papers from scientific and technical conferences, symposia, seminars, or other meetings sponsored or cosponsored by NASA.

- SPECIAL PUBLICATION. Scientific, technical, or historical information from NASA programs, projects, and missions, often concerned with subjects having substantial public interest.

- TECHNICAL TRANSLATION. English-language translations of foreign scientific and technical material pertinent to NASA's mission.

Specialized services that complement the STI Program Office's diverse offerings include creating custom thesauri, building customized databases, organizing and publishing research results . . . even providing videos.

For more information about the NASA STI Program Office, see the following:

- Access the NASA STI Program Home Page at ***http://www.sti.nasa.gov***

- E-mail your question via the Internet to help@sti.nasa.gov

- Fax your question to the NASA Access Help Desk at 301–621–0134

- Telephone the NASA Access Help Desk at 301–621–0390

- Write to:
  NASA Access Help Desk
  NASA Center for AeroSpace Information
  7121 Standard Drive
  Hanover, MD 21076

NASA/TM—2002-211104

Ultrasonic Resonance Spectroscopy of Composite Rims for Flywheel Rotors

Laura M. Harmon
Cleveland State University, Cleveland, Ohio

George Y. Baaklini
Glenn Research Center, Cleveland, Ohio

Prepared for the
28th Annual Review of Progress in Quantitative Nondestructive Evaluation (QNDE)
sponsored by the Center for Nondestructive Evaluation, Iowa State University
Brunswick, Maine, July 29–August 3, 2001

National Aeronautics and
Space Administration

Glenn Research Center

September 2002

Available from

NASA Center for Aerospace Information
7121 Standard Drive
Hanover, MD 21076

National Technical Information Service
5285 Port Royal Road
Springfield, VA 22100

Available electronically at http://gltrs.grc.nasa.gov

Ultrasonic Resonance Spectroscopy of Composite Rims for Flywheel Rotors

Laura M. Harmon
Cleveland State University
Cleveland, OH 44115

George Y. Baaklini
National Aeronautics and Space Administration
Glenn Research Center
Cleveland, OH 44135

Summary

Flywheel energy storage devices comprising multilayered composite rotor systems are being studied extensively for utilization in the International Space Station. These composite material systems were investigated with a recently developed ultrasonic resonance spectroscopy technique. The ultrasonic system employs a continuous swept-sine waveform and performs a fast Fourier transform (FFT) on the frequency response spectrum. In addition, the system is capable of equalizing the amount of energy at each frequency. Equalization of the frequency spectrum, along with interpretation of the second FFT, aids in the evaluation of the fundamental frequency. The frequency responses from multilayered material samples, with and without known defects, were analyzed to assess the capabilities and limitations of this nondestructive evaluation technique for material characterization and defect detection. Amplitude and frequency changes were studied from ultrasonic responses of thick composite rings and a multiring composite rim. A composite ring varying in thickness was evaluated to investigate the full thickness resonance. The frequency response characteristics from naturally occurring voids in a composite ring were investigated. Ultrasonic responses were compared from regions with and without machined voids in a composite ring and a multiring composite rim. Finally, ultrasonic responses from the multiring composite rim were compared before and after proof spin testing to 63,000 rpm.

Introduction

Flywheel energy storage devices comprising multilayered composite rotor systems generate and store energy in a rotating mass. The rotor is the complete rotating assembly of the flywheel, primarily composed of a metallic hub and a composite rim, as shown in figure 1. The rim, as illustrated in figure 1, may contain several concentric composite rings with varying composite materials and geometries. Thick composite rings and a multiring composite rim such as these were investigated in this study for use in International Space Station (ISS) flywheel systems.

Ultrasonic spectroscopy is used in the nondestructive evaluation (NDE) of materials. Previous approaches to ultrasonic spectroscopy demonstrated its effectiveness in evaluating attenuation, velocity, and degradation in composite materials and ceramics; detecting and classifying discrete flaws, cracks, and corrosion; characterizing delaminations in composites; and analyzing multiple-layered structures and adhesively bonded joints (refs. 1 to 4). A narrow ultrasonic signal was pulsed into a specimen with a piezoelectric broadband transducer, creating a wide bandwidth frequency response. After ultrasound traveled through a specimen, a broadband transducer received the ultrasonic response in the time domain. A spectrum analyzer converted the ultrasonic pulse from the time domain to the frequency domain with a fast Fourier transform (FFT). The resulting spectrum was analyzed for amplitude and frequency changes. For more details, the reader should consult the extensive review of previous approaches to ultrasonic spectroscopy and its applications produced by Fitting and Adler (ref. 2).

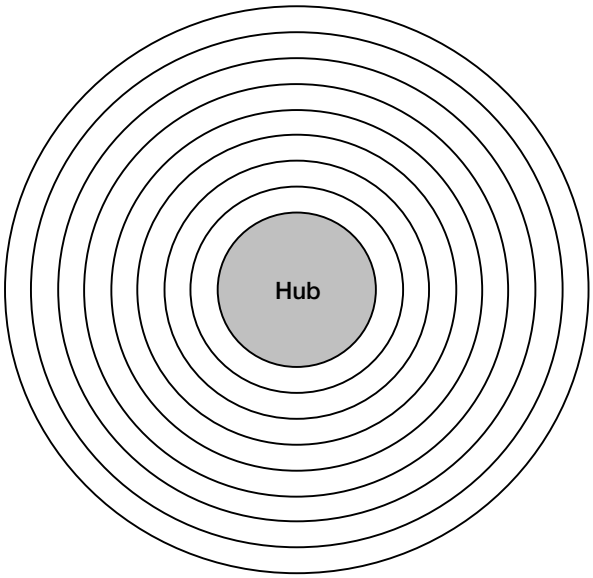

Figure 1.—Rotor showing metallic hub with rim consisting of eight concentric rings.

Tucker (ref. 5) developed and patented a new approach to ultrasonic spectroscopy called ultrasonic resonance spectroscopy (URS). This system utilizes a continuous swept-frequency waveform in a pitch-catch or through-transmission mode. The technique requires performing an additional FFT on the frequency spectrum to find the fundamental resonant frequencies or spectrum resonance spacing, which result from a localized ultrasonic standing wave existing in a plate.

This method exhibited more advances in detecting hidden corrosion in aluminum plates (ref. 6) and evaluating bond quality in multiple-layered structures (ref. 7) than previously used techniques. In addition, the method was able to evaluate thin and thick multilayered composite rings from flywheels for the ISS (ref. 8). The system also showed potential as a scanning technique (ref. 9).

The current study assessed the limitations and capabilities of URS as an NDE technique for material characterization and defect detection. Amplitude and frequency changes in the spectrum and spectrum resonance spacing domains were evaluated from the ultrasonic responses of thick composite rings and a multiring composite rim. A thick composite ring with varying thickness was analyzed to investigate the full thickness resonance capabilities. The responses from areas in rings with manufactured and naturally occurring voids were compared to those from defect-free areas. A multiring composite rim with electrical discharge machining (EDM) notches was evaluated to determine the capabilities and limitations in detecting defects in the rim. Finally, the multiring composite rim was investigated before and after proof spin testing to 63,000 rpm to establish baseline data for further investigation.

Background

Resonance

The fundamental resonant frequency results from a localized ultrasonic standing wave existing in a specimen whose thickness is equal to half of the wavelength. The fundamental resonant frequency is calculated from an equation that relates frequency to the thickness of and acoustic velocity in a plate. The fundamental relation (ref. 4) between the frequency f, wavelength λ, and acoustic velocity c is

$$c = f\lambda \tag{1}$$

Rearranging these terms yields

$$f = \frac{c}{\lambda} \tag{2a}$$

At the fundamental resonant frequency f_R, there is a half wavelength in the plate thickness and

$$d = \frac{\lambda}{2} \tag{2b}$$

where d is the plate thickness. Solving for the wavelength λ yields

$$\lambda = 2d \tag{3}$$

Substituting equation (3) into equation (2) yields

$$f_R = \frac{c}{2d} \tag{4}$$

Ultrasonic System

The commercially available ultrasonic system (ref. 5) employed in the current analysis includes a digital processing oscilloscope, amplifier, digital-to-analog converter, and necessary computer software. The software generates a continuous swept-frequency acoustic wave and captures the frequency response of a test specimen. The frequency sweep or interval is user defined, with capabilities from the audible range to 8 MHz (James Tucker, in July 1999 E-mail to Laura Harmon). Figure 2 depicts the URS process with the ultrasonic system. The computer software generates a digital-input waveform, shown in figure 2(a). The digital-input waveform is converted to an analog signal and transmitted into the test specimen with a medium-damped direct-contact transducer. The medium-damped transducer maintains a high level of energy while providing a wide-bandwidth frequency response. Another medium-damped transducer receives the ultrasonic response in the time domain, shown in figure 2(b). A digital spectrum analyzer converts the ultrasonic wave from the time domain to the frequency domain via FFT, shown in figure 2(c). The frequency spectrum contains higher order resonance peaks or harmonics, as exhibited by the material system under investigation. Since the value of each harmonic is an integer multiple of the fundamental frequency, the fundamental frequency is represented by the spacing between resonance peaks. Consequently, the performance of a second FFT on the spectrum produces a peak representing the spectrum resonance spacing, or the fundamental resonant frequency, as shown in figure 2(c). A resonance peak in the spectrum resonance spacing domain indicates an impedance mismatch.

To eliminate the effects of a nonlinear transducer response, the system has the capability of equalizing the amount of energy distributed to each frequency. Equalization is accomplished by coupling the transducers face to face, as illustrated in figure 3(a). An example of the resulting input spectrum after equalization is shown in figure 3(b). To compensate for the energy lost through attenuation, as in the present study, more energy can be devoted to the higher frequencies with the resulting energy distribution depicted in figure 3(c).

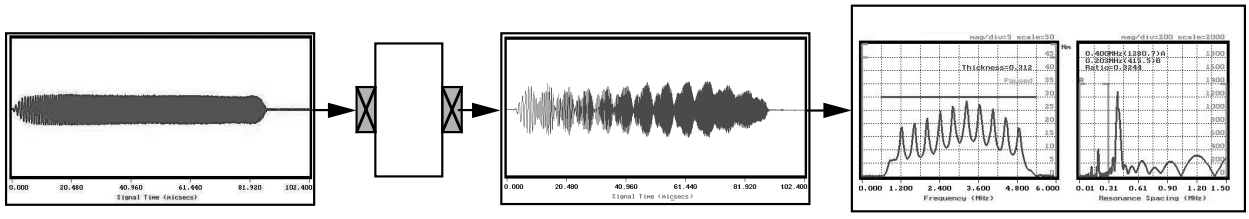

Figure 2.—Through-transmission ultrasonic spectroscopy on Lucite sample. (a) Digital input waveform in time domain. (b) Digital output waveform in time domain. (c) Typical output display.

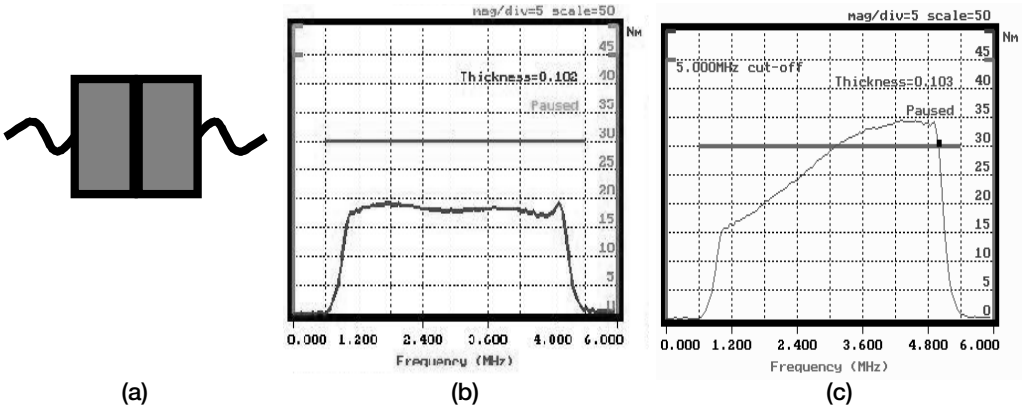

Figure 3.—Equalization process. (a) Two transducers held face to face. (b) Spectrum providing equal amounts of energy to each frequency. (c) Spectrum providing greater amounts of energy to higher frequencies.

Specimens and Experimental Procedures

Specimens

Four specimens, three composite rings and a multiring composite rim, were considered in this study. The thick composite rings Log Drop 1.4, STD 3, and R2.6 had very similar structures. Evaluation of Log Drop 1.4 investigated changes in resonant frequencies due to thinning of various sections. Sections were milled from the ring, as shown in figure 4. Region (a) of the ring was left intact; one section was removed from (b); and increasingly thick sections were milled from regions (c), (d), and (e). Intentionally manufactured EDM notches and drilled holes of varying sizes and depths were placed throughout the STD 3 ring. Ultrasonic responses were compared from regions with and without manufactured flaws to observe changes in amplitude and resonant frequency. Ring R2.6 exhibited regions that were affected by unintentional manufacturing flaws. Figure 5 shows three locations of interest in Ring R2.6: (a) a defect-free region; (b) a 1.0-mm (0.04-in.) void in the ring spanning 4.1 mm (0.16 in.) perpendicular to the ultrasonic wave path; and (c) a void cluster 7.7 mm (0.3 in.) in the ring spanning 12.2 mm (0.48 in.), also perpendicular to the ultrasonic wave path.

The multiring composite rim consisted of multiple concentric rings similar to the thick composite rings. The rim was evaluated before and after proof spin testing to 63,000 rpm. Before spin testing, a section of the rim was removed. EDM notches and drilled holes of different sizes and at different locations were machined into this section of the rim, also known as the standard rim. Responses from areas with and without detectable EDM notches on the standard rim were compared. After spin testing of the rim free of EDM notches, measurements were taken along the circumference every 45° in the counterclockwise direction, starting at 0° with one measurement at 15°. These responses were compared to the responses from the areas of the standard rim section without detectable EDM notches for evaluation before and after spin testing.

Experimental Procedures

All specimens were evaluated in the pitch-catch (i.e., send-receive) mode of ultrasonic transmission with direct contact. The transducers were coupled to the outer diameter of the rings with couplant A (propylene glycol) or couplant D (gel). Coaxial cables connected the transducers to the transmitter and receiver. Medium-damped transducers maximized energy while keeping the bandwidth broad.

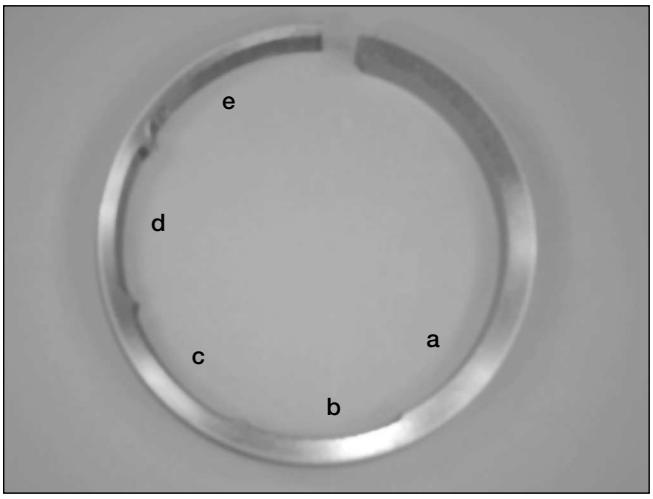

Figure 4.—Ring Log Drop 1.4 with composite sections removed, where region (a) remained intact; (b) had one section removed; and (c), (d), and (e) had increasingly thick sections removed.

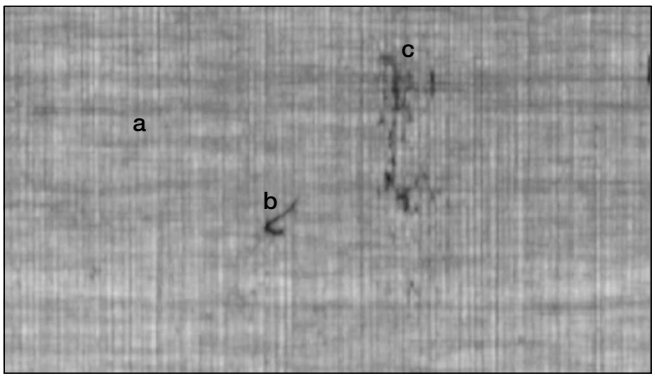

Figure 5.—Ultrasonic C-scan of section of Ring R2.6 showing presence of (a) unflawed region, (b) void 1.0 mm into ring, and (c) void cluster 7.7 mm into ring.

Results and Analysis

Ring Log Drop 1.4

Figure 6 compares the response for section (c) with a thickness of 7.72 mm (0.304 in.) to the response for section (a) with a thickness of 10.87 mm (0.428 in.). Only the full thickness resonances were present at 0.198 MHz for region (c) and 0.144 MHz for region (a) in the spectrum resonance spacing domain. These responses are typical of the ultrasonic responses for each region of the ring. Resonant frequencies corresponding to locations within the thickness were not present in the spectrum resonance spacing domain, indicating that the full thickness resonated as one system and that the system was well bonded. The graph in figure 7 illustrates spectrum resonance spacing versus thickness, showing the resonant frequencies at each region of the ring. As expected, thinner regions produced larger resonant frequencies.

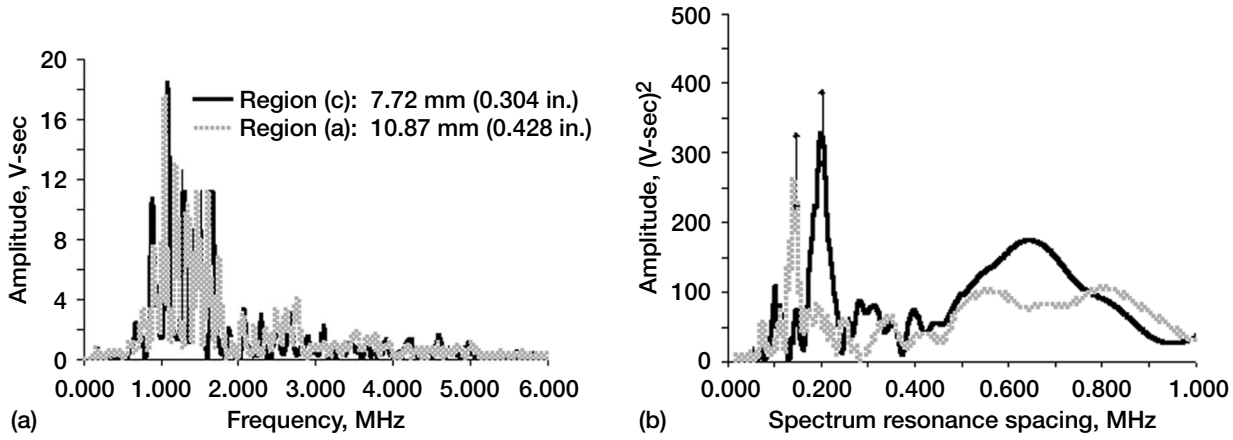

Figure 6.—Ultrasonic data from two regions of Ring Log Drop 1.4. (a) Spectrum. (b) Spectrum resonance spacing.

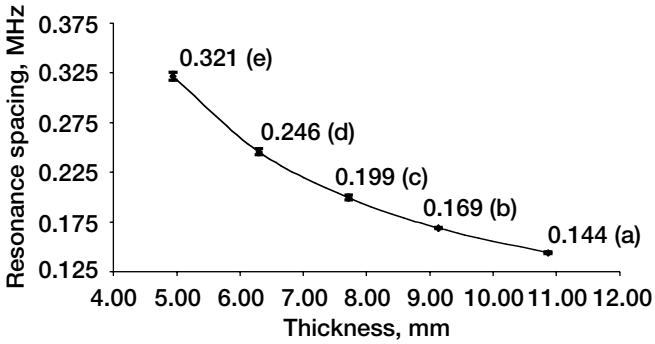

Figure 7.—Resonance at regions (a) to (e) of Ring Log Drop 1.4.

Ring STD 3

Figures 8, 9, and 10 compare the ultrasonic response from a defect-free region to the responses from regions with three manufactured flaws greater than or equal to 1.7 mm (0.07 in.) in width perpendicular to the ultrasonic wave path. For the defect-free regions of STD 3, a sharp peak appeared at 0.148 ± 0.008 MHz, representing the full thickness of 10.74 mm (0.423 in.) resonating. In addition, there was a resonance peak at 0.214 MHz, which corresponds to the thickness of 7.64 mm (0.301 in.). Sharp peaks indicate high impedance mismatches; however, Ring Log Drop 1.4 did not produce multiple sharp peaks in the spectrum resonance spacing. These facts suggest the existence of a kissing disbond (i.e., close mechanical contact without bonding) in STD 3 approximately 7.64 mm (0.301 in.) into the ring. Energy traveled through the ring to resonate the full thickness of the ring, as well as part of the full thickness. A previous study (ref. 7) suggested that such resonances may be indicative of a bonded sample where some energy penetrates the bond to resonate the full thickness of the sample, and some energy reflects at the bond. Therefore, a position at 7.64 mm (0.301 in.) into STD 3 may have a weaker bond than other locations nearer the outer diameter. Optically, degradation cannot be seen at the depth of 7.64 mm (0.301 in.) into the ring. In addition, real-time x-ray, ultrasonic C-scan, and computed tomography scans did not detect damage at this location. Further investigation is required to determine whether URS detected a kissing disbond or a weak bond that went undetected by other NDE methods.

The three responses from regions with defects of widths greater than or equal to 1.7 mm (0.07 in.) perpendicular to the ultrasonic wave path indicated amplitude reductions in both the spectrum and spectrum resonance spacing domains. The locations of the defects were not determined from the responses, as resonances corresponding to the

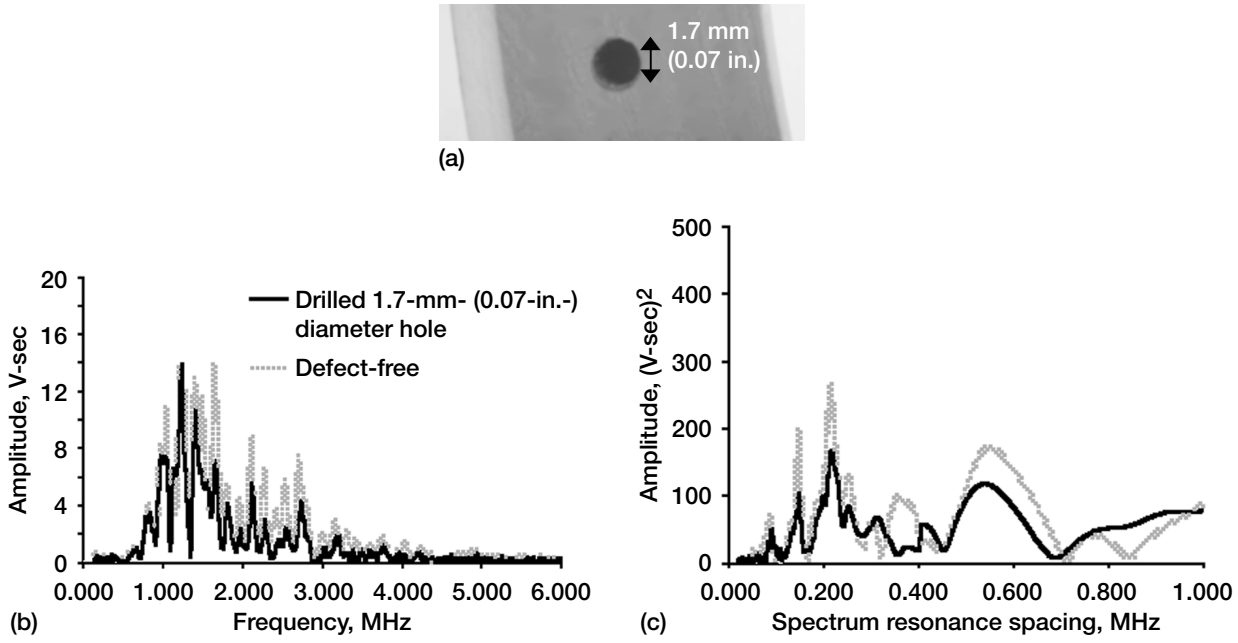

Figure 8.—(a) Optical photograph of 1.7-mm- (0.07-in.-) diameter drilled hole in Ring STD 3 with ultrasonic data comparing (b) frequency spectrum and (c) spectrum resonance spacing from defect-free region to region with drilled hole.

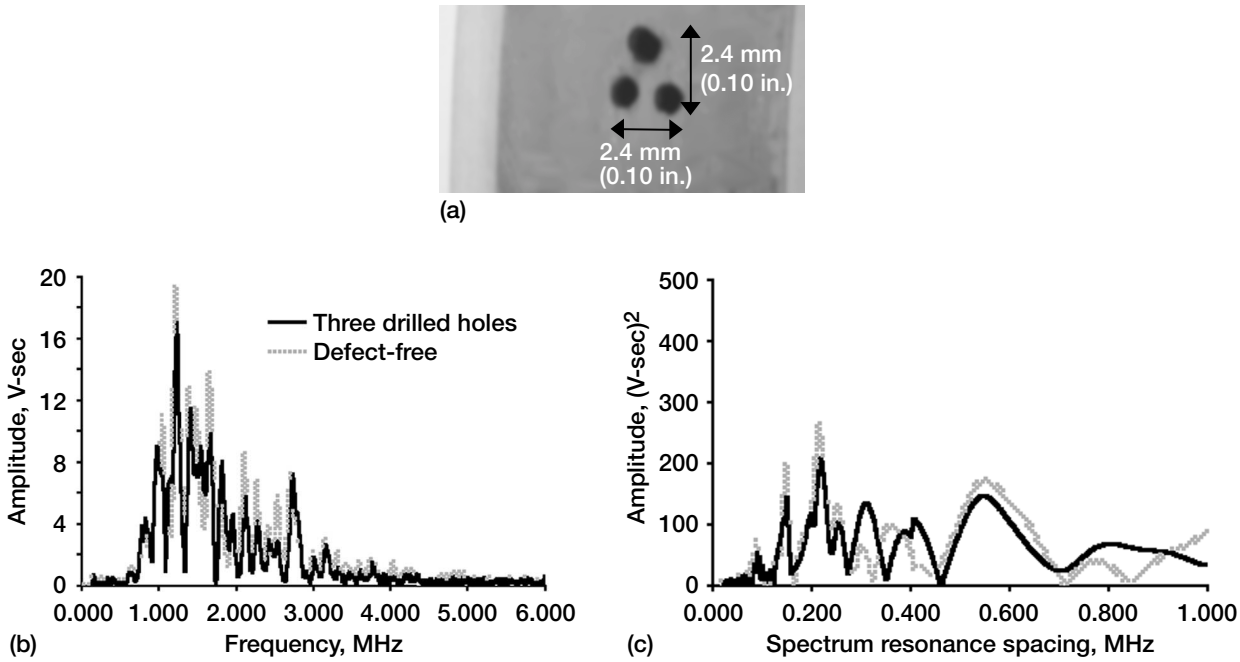

Figure 9.—(a) Optical photograph of three drilled holes in Ring STD 3 with ultrasonic data comparing (b) frequency spectrum and (c) spectrum resonance spacing from defect-free region to region with three drilled holes.

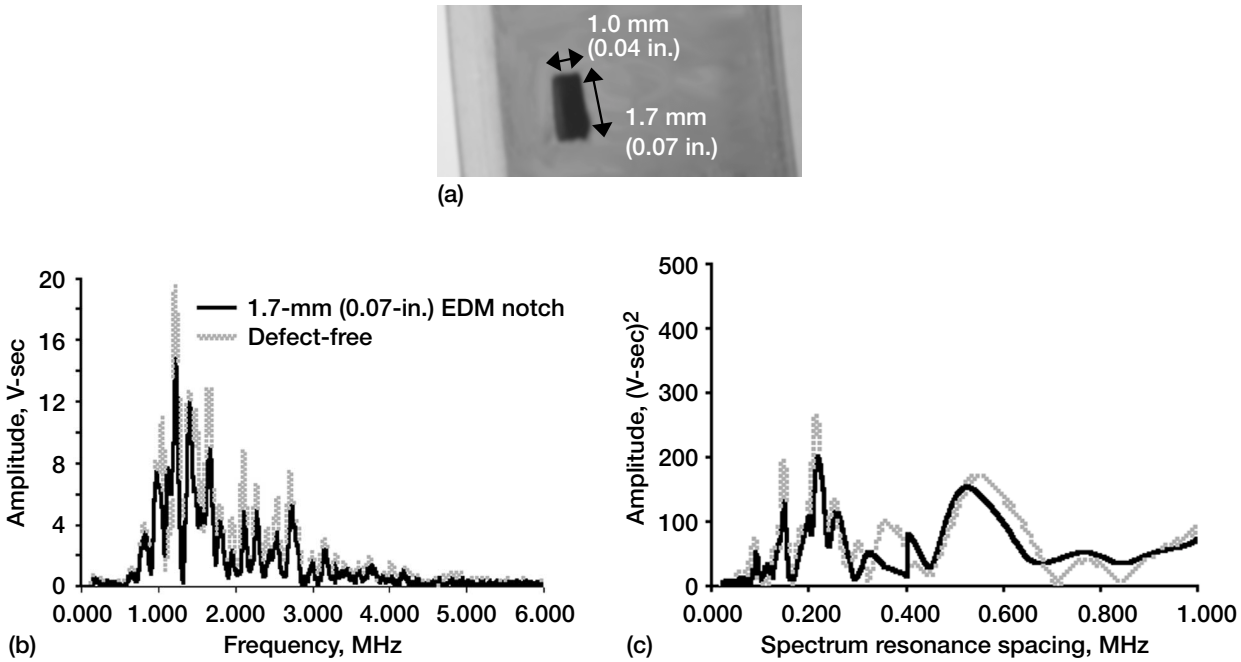

Figure 10.—(a) Optical photograph of 1.7-mm (0.07-in.) by 1.0-mm (0.04-in.) EDM notch in Ring STD 3 with (b) frequency spectrum and (c) spectrum resonance spacing comparing EDM notch to defect-free region.

location of the flaws did not consistently appear. The only signal that may have indicated the location of the flaw is shown in figure 9. A resonance peak increased in amplitude at 0.309 MHz, which corresponds to the location of the porosity network of drilled holes.

Hence, URS detected discrete defects with widths greater than or equal to 1.7 mm (0.07 in.) perpendicular to the ultrasonic wave path as a reduction of amplitude in the spectrum and spectrum resonance spacing domains. The locations of the defects were not determined, as resonance peaks corresponding to the locations did not consistently appear.

Ring R2.6

Figure 11 compares responses from the defect-free region and the region with the 4.1-mm- (0.16-in.-) wide void 1 mm (0.04 in.) from the outer diameter. For the defect-free region, a sharp peak was present at 0.118 ± 0.008 MHz representing the full thickness resonance. In addition to the full thickness resonance, a sharp peak at 0.157 ± 0.008 MHz appeared, representing an approximate thickness of 9.6 mm (0.38 in.) from the outer diameter of the ring. This resonance may be indicative of a kissing disbond at the corresponding location; further investigation of the results are needed to corroborate its existence. Less-defined peaks at 0.248, 0.312, and 0.494 MHz, corresponding to the approximate thicknesses of 6.1 mm (0.24 in.), 5.5 mm (0.22 in.), and 4 mm (0.16 in.) from the outer diameter, emerged in the response for the defect-free region as well. Further NDE is necessary to verify the source of the resonance peaks, as computed tomography did not locate defects at these locations (see figs. 11(c) and 12(c)).

The void in figure 11(c) produced the ultrasonic response also shown in figure 11. The fundamental resonant frequency corresponding to the location of the void was not resolved in the spectrum resonance spacing domain because the spectrum sweep or interval was capable of exciting the fundamental frequency only. For a resonance to be resolved in the spectrum resonance spacing domain, more than one peak is necessary in the spectrum domain. Due to time constraints, another wider sweep was not performed. However, there were observable changes in the

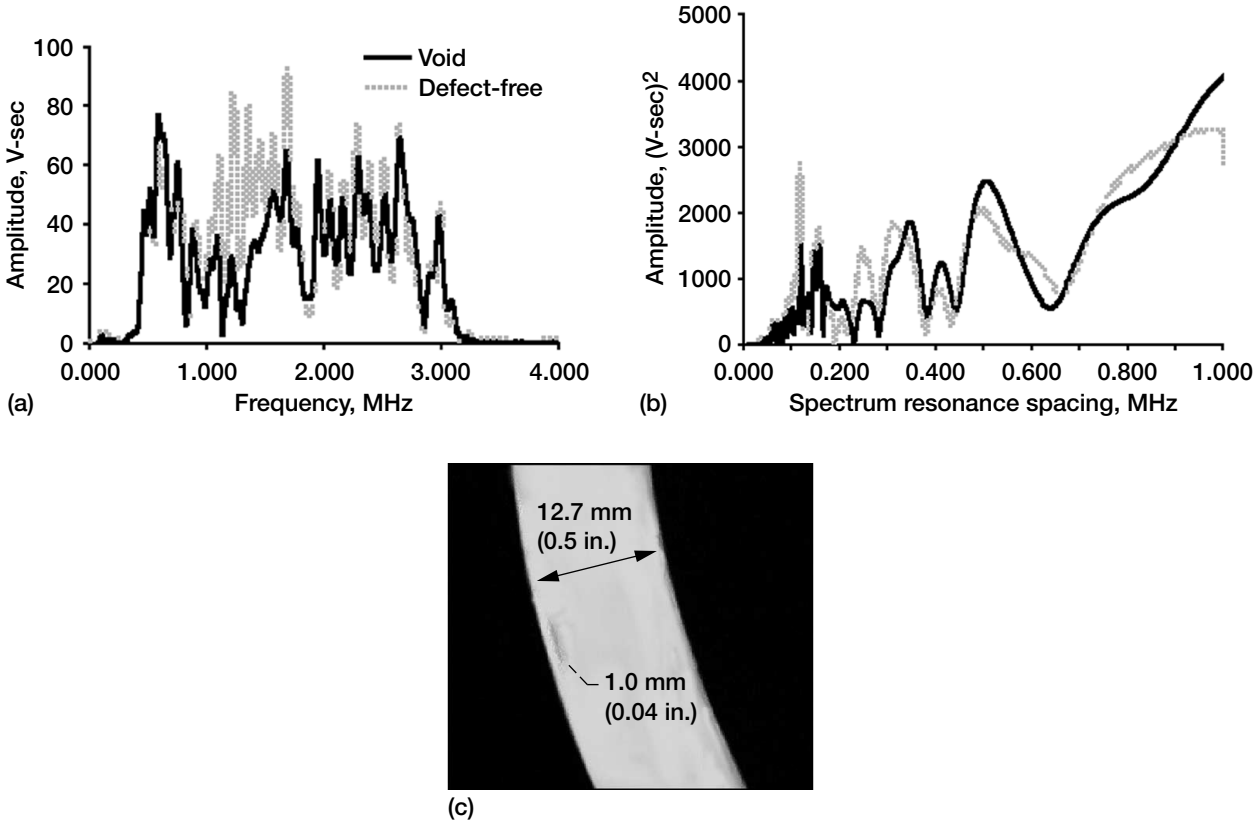

Figure 11.—Regions with and without void 1.0 mm into ring R2.6. (a) Spectrum. (b) Spectrum resonance spacing. (c) Computed tomography image showing location of void.

response. The amplitude of the full thickness resonance at 0.118 MHz decreased by approximately 40 percent, which means that less energy returned through the full thickness. The resonant frequency at 0.147 MHz shifted outside the error of the 0.157 MHz resonance but remained at the same amplitude. In addition, there was an overall amplitude reduction in the frequency spectrum. A resonance corresponding to the location of the void, 1.0 mm (0.04 in.) from the outer diameter of ring R2.6, was not resolved in the spectrum resonance spacing.

Figure 12 compares responses for the defect-free region and the region with the void cluster 7.7 mm (0.3 in.) into the ring spanning 12.2 mm (0.48 in.) perpendicular to the ultrasonic wave path. The resonance corresponding to the location of the void cluster, 0.210 MHz, did not emerge in the response in figure 12. The amplitude of the full thickness resonance declined by approximately 60 percent. In addition, the frequency spectrum indicated amplitude reductions of approximately 60 percent for the frequencies beyond 1.800 MHz. Therefore, URS evaluation detected the presence of damage only by a reduction in amplitude.

Multiring Composite Rim With Manufactured Flaws at Different Locations

Results from the standard rim with manufactured flaws indicated that URS did not detect or locate discrete notches with a width of 1.5 mm (0.06 in.) perpendicular to the ultrasonic wave path because of scattering and dispersion. In contrast to Ring STD 3 and Ring R2.6, changes in amplitude were not observed because the notches in the rim were smaller than those in the rings. In addition, resonances corresponding to the locations of the defects did not appear.

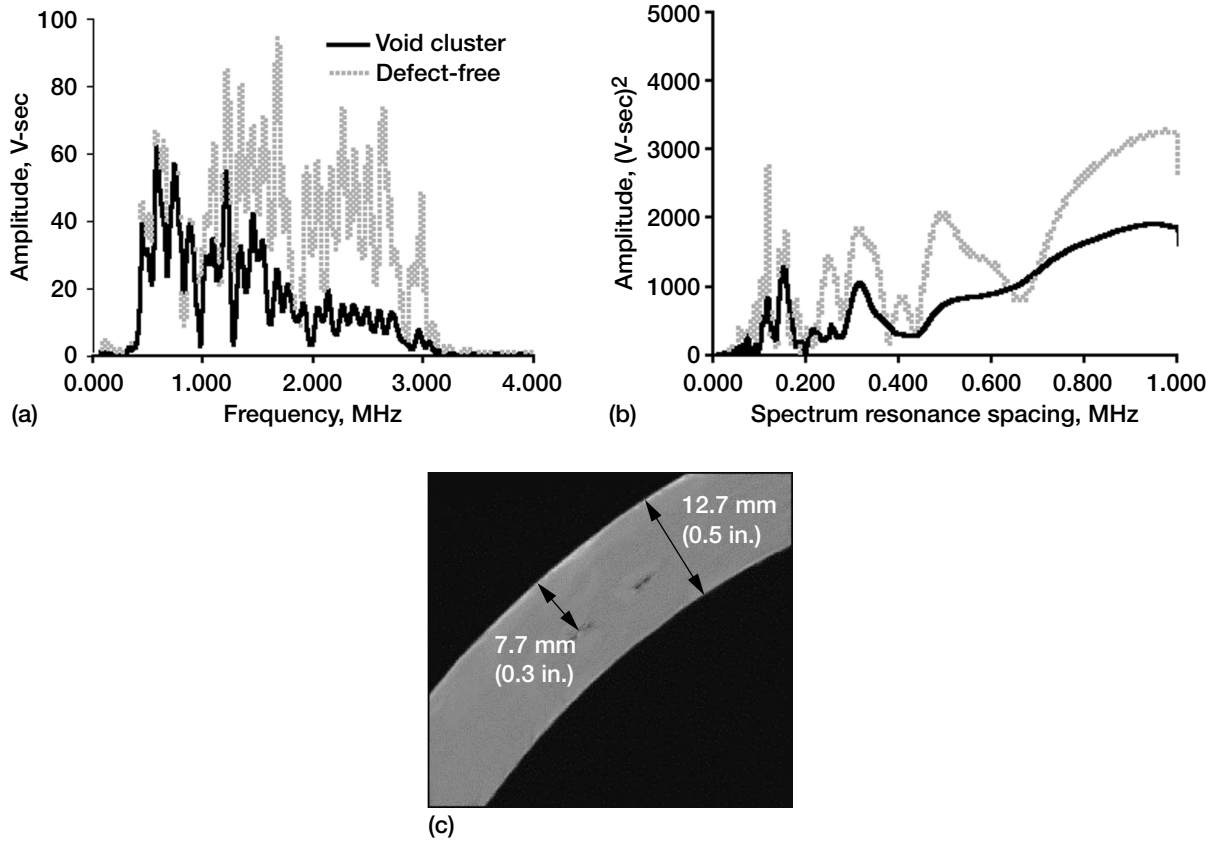

Figure 12.—Void cluster in Ring R2.6. (a) Spectrum. (b) Spectrum resonance spacing. (c) Computed tomography image.

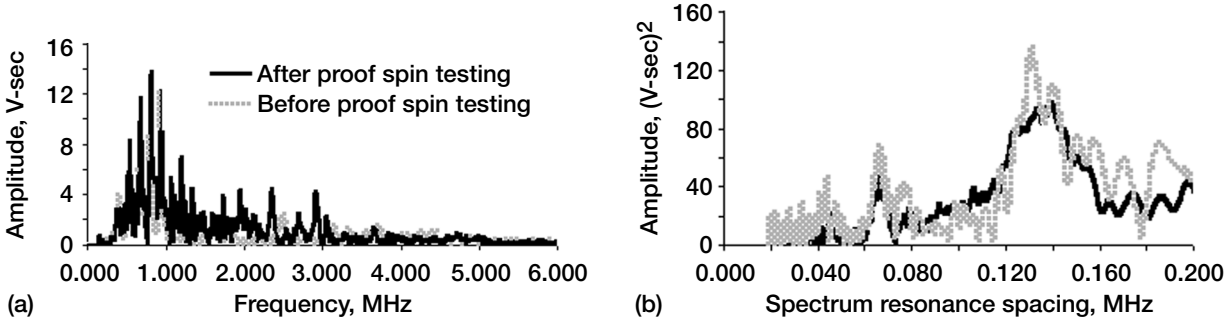

Figure 13.—Ultrasonic data from multiring composite rim before and after proof spin testing. (a) Spectrum. (b) Spectrum resonance spacing.

Multiring Composite Rim Before and After Proof Spin Testing

Figure 13 compares two URS responses before and after proof spin testing. The resonance for the full thickness of the rim, 82.0 mm (3.23 in.), was calculated as 0.019 MHz. The full thickness resonance did not appear in the ultrasonic response, as expected, because ultrasound previously had penetrated only 48 mm into this rim (ref. 10). The largest resonance peak appearing in the spectrum resonance spacing domain in figure 13(b) had two parts for both ultrasonic responses. The resonance of the highest amplitude occurred at approximately 0.142 MHz, corresponding to 11.2 mm (0.44 in.), whereas the lower amplitude resonance occurred at approximately 0.132 MHz, corresponding to 12.1 mm (0.48 in.). The thickness of the outer ring was 12.0 mm (0.47 in.). These measurements and calculations suggested that the outer ring resonated. Additional resonances appeared at 0.033, 0.045, and 0.066 MHz, shown in figure 13, corresponding to 48.2 (1.90 in.), 36.2 (1.43 in.), and 23.7 mm (0.93 in.) from the outer diameter of the rim. These resonances appeared in all the responses at varying amplitudes, before and after spin testing. Their thicknesses correspond to the thickness from the outer diameter to the fourth ring at 48 mm, third ring at 36 mm, and second ring at 24 mm, respectively.

The fact that the URS responses for the rim before and after spin testing contained the same resonance peaks suggests that spin testing did not introduce damage into the outer four rings of the rim. Results were in agreement with results from ultrasonic pulse-echo scans and x-ray tomography. These URS responses will be used in the future as signatures for rims of the same structure. Any damage existing within 48 mm of the rotor may be detected using these signatures. Future analysis of the URS data from this rim will investigate any damage that may occur due to fatigue testing.

URS did show potential in evaluating composite rims, as the signals before and after proof spin testing contained detailed resonances for the outer four rings. The signals acquired will serve as baseline, or signature, signals for further evaluation and analysis of the composite rim. The appearance or disappearance of resonances, along with changes in amplitude, will be monitored to investigate the damage state of the outer rings of the rim. This type of analysis will improve the qualification, certification, and lifing of composite rims because these rims are designed with a fail-safe system: when an outer ring disbonds, the flywheel rotor goes out of balance, causing a system shutdown.

Summary of Findings

URS detected the full thickness resonance in a well-bonded thick composite ring with a single resonance in the spectrum resonance spacing domain. In addition, full thickness resonances increased in value as the thickness decreased in different sections of the composite ring.

Evaluation of the composite standard ring with intentional EDM notches and drilled holes demonstrated that discrete voids greater than or equal to 1.70 mm in width perpendicular to the ultrasonic wave path were detected as an amplitude reduction in the amplitude of the spectrum and spectrum resonance spacing when compared to a defect-free region. The locations of discrete voids were not consistently determined, since resonances corresponding to their locations within the thickness did not appear in the spectrum resonance spacing domain. Data from the thick composite ring also contained resonances at locations with possible kissing disbonds that were not detected by other NDE methods.

Data from naturally occurring single and clustered voids in a thick composite ring indicated that a single 4.1-mm- (0.16-in.-) wide and 0.8-mm- (0.03-in.-) thick void 1.0 mm below the surface caused a 40-percent reduction in the full thickness resonance in the spectrum resonance spacing domain and a general decrease in the spectrum domain. Clustered voids 7.7 mm below the surface reduced the amplitudes of the full thickness resonance in the spectrum resonance spacing domain by 60 percent. Frequencies above 1.800 MHz in the spectrum domain declined by 60 percent. However, the locations of the single void and the void cluster were not detected. In addition, ultrasonic data detected possible kissing disbonds that were undetected by other NDE methods.

A comparison of URS responses from a rim made of concentric composite rings with and without EDM notches and drilled holes detected minimal differences between responses. The amplitude changes observed in the URS responses of the rings were not observed in the responses for the rim because the notches in the rim were smaller

than those detected in the rings. The URS response detected resonant frequencies corresponding to the location of the four outer rings, which will be used to monitor the damage state of the rim during its life. The full thickness resonance of the standard rim was not detected because sound penetration was limited to 48 mm into the rim. The URS response from the composite rim before and after spin testing to 63,000 rpm produced resonances of similar amplitude and frequency, indicating the successful manufacturing of a multiring composite rim. This was in agreement with results from ultrasonic pulse-echo scans and x-ray tomography NDE by other researchers.

Conclusion

Multilayered composite rotor systems were investigated with ultrasonic resonance spectroscopy (URS) to assess capabilities and limitations for flaw detection and material characterization. Amplitude and frequency changes in the spectrum and spectrum resonance spacing domains were evaluated to establish the foundation for characterizing the damage state in a composite rotor and related material systems targeted for flywheel technology of the International Space Station.

This study assessed the capabilities and limitations of URS as an NDE method for flywheel composite rotor evaluation. The full thickness resonance was produced in a defect-free composite ring. The presence of discrete and clustered voids with a width greater than 1.70 mm (0.067 in.) perpendicular to the ultrasonic wave path was detected in composite rings as an amplitude reduction in the spectrum and spectrum resonance spacing. The unique detection of kissing disbonds by URS requires further investigation, since their existence in the composite rings and rims was not confirmed destructively or corroborated with other nondestructive techniques. Voids of a width of 1.5 mm (0.06 in.) were not detected in the multiring composite rim. The presence of the four outer rings was detected, as resonances corresponding to their locations appeared. The responses before and after spin testing contained the same resonances for the four outer rings, suggesting that damage was not introduced to the rim by proof spin testing. As a result, the signals acquired from the multiring composite rim will be baseline signatures for comparison with signals after fatigue testing. Based on these findings, URS is a viable tool for flight certification of flywheel rotors to be used in the International Space Station.

References

1. Birks, Albert S.; Green, Robert E., Jr.; and McIntire, Paul: Ultrasonic Testing. American Society for Nondestructive Testing, Columbus, OH, 1991.
2. Fitting, Dale W.; and Adler, Laszlo: Ultrasonic Spectral Analysis for Nondestructive Evaluation. Plenum Press, New York, NY, 1981.
3. Gericke, O.R.: Ultrasonic Spectroscopy. Research Techniques in Nondestructive Testing, ch. 2, R.S. Sharpe, ed., Academic Press, London, England, 1970.
4. Krautkramer, Josef; and Krautkramer, Herbert: Ultrasonic Testing of Materials. 2nd ed., Springer-Verlag, New York, NY, 1977.
5. Tucker, James R.: Apparatus and Method for Ultrasonic Spectroscopy Testing of Materials. U.S. Patent 5,591,913, January 7, 1997.
6. Tucker, James R.: Ultrasonic Spectroscopy for Corrosion Detection and Multiple Layer Bond Inspection. Proceedings of the First Joint DoD/FAA/NASA Conference on Aging Aircraft, vol. II, 1998, pp. 1537–1550.
7. Chambers, J.K.; and Tucker, J.R.: Bondline Analysis Using Swept-Frequency Ultrasonic Spectroscopy. Insight, vol. 41, no. 3, 1999, pp. 151–155.
8. Harmon, Laura M.; and Baaklini, George Y.: Ultrasonic Resonance Spectroscopy of Composite Rings for Flywheel Rotors. Nondestructive Evaluation of Materials and Composites V: Proceedings of SPIE vol. 4336, 2001.
9. Martin, Richard; and Baaklini, George Y.: Scanning Ultrasonic Spectroscopy for Composite Flywheels. Nondestructive Evaluation of Materials and Composites V: Proceedings of SPIE, vol. 4336, 2001.
10. Baaklini, George Y., et al.: NDE Methodologies for Composite Flywheels Certification. NASA/TM—2000-210473, 2000. http://gltrs.grc.nasa.gov/GLTRS/ Accessed September 9, 2001.

REPORT DOCUMENTATION PAGE

Form Approved
OMB No. 0704-0188

1. AGENCY USE ONLY (*Leave blank*)	2. REPORT DATE	3. REPORT TYPE AND DATES COVERED
	September 2002	Technical Memorandum

4. TITLE AND SUBTITLE

Ultrasonic Resonance Spectroscopy of Composite Rims for Flywheel Rotors

5. FUNDING NUMBERS

WU–755–1A–09–00

6. AUTHOR(S)

Laura M. Harmon and George Y. Baaklini

7. PERFORMING ORGANIZATION NAME(S) AND ADDRESS(ES)

National Aeronautics and Space Administration
John H. Glenn Research Center at Lewis Field
Cleveland, Ohio 44135–3191

8. PERFORMING ORGANIZATION REPORT NUMBER

E–12949

9. SPONSORING/MONITORING AGENCY NAME(S) AND ADDRESS(ES)

National Aeronautics and Space Administration
Washington, DC 20546–0001

10. SPONSORING/MONITORING AGENCY REPORT NUMBER

NASA TM—2002-211104

11. SUPPLEMENTARY NOTES

Prepared for the 28th Annual Review of Progress in Quantitative Nondestructive Evaluation (QNDE) sponsored by the Center for Nondestructive Evaluation, Iowa State University, Brunswick, Maine, July 29–August 3, 2001. Laura M. Harmon, Cleveland State University, Cleveland, Ohio 44115, and George Y. Baaklini, NASA Glenn Research Center. Responsible person, George Y. Baaklini, organization code 5920, 216–433–6016.

12a. DISTRIBUTION/AVAILABILITY STATEMENT

Unclassified - Unlimited
Subject Categories: 38 and 20 Distribution: Nonstandard

Available electronically at http://gltrs.grc.nasa.gov

This publication is available from the NASA Center for AeroSpace Information, 301–621–0390.

12b. DISTRIBUTION CODE

13. ABSTRACT ***(Maximum 200 words)***

Flywheel energy storage devices comprising multilayered composite rotor systems are being studied extensively for utilization in the International Space Station. These composite material systems were investigated with a recently developed ultrasonic resonance spectroscopy technique. The ultrasonic system employs a continuous swept-sine waveform and performs a fast Fourier transform (FFT) on the frequency response spectrum. In addition, the system is capable of equalizing the amount of energy at each frequency. Equalization of the frequency spectrum, along with interpretation of the second FFT, aids in the evaluation of the fundamental frequency. The frequency responses from multilayered material samples, with and without known defects, were analyzed to assess the capabilities and limitations of this nondestructive evaluation technique for material characterization and defect detection. Amplitude and frequency changes were studied from ultrasonic responses of thick composite rings and a multiring composite rim. A composite ring varying in thickness was evaluated to investigate the full thickness resonance. The frequency response characteristics from naturally occurring voids in a composite ring were investigated. Ultrasonic responses were compared from regions with and without machined voids in a composite ring and a multiring composite rim. Finally, ultrasonic responses from the multiring composite rim were compared before and after proof spin testing to 63,000 rpm.

14. SUBJECT TERMS

Ultrasonic spectroscopy; Spectrum analysis; Resonance; Resonant frequencies; Composite materials; Flywheels; Rotors; Nondestructive tests

15. NUMBER OF PAGES

18

16. PRICE CODE

17. SECURITY CLASSIFICATION OF REPORT	18. SECURITY CLASSIFICATION OF THIS PAGE	19. SECURITY CLASSIFICATION OF ABSTRACT	20. LIMITATION OF ABSTRACT
Unclassified	Unclassified	Unclassified	